Polyelectrolyte−Colloid Complexes: Polarizability and Effective Interaction

J. Dzubiella,*,†,‡,§ A. G. Moreira,‡ and P. A. Pincus‡,||

Institut für Theoretische Physik II, Heinrich-Heine-Universität Düsseldorf, Universitätsstrasse 1, D-40225 Düsseldorf, Germany, Materials Research Laboratory, University of California, Santa Barbara, Santa Barbara, California 93106, Kavli Institute for Theoretical Physics, Kohn Hall, University of California, Santa Barbara, California 93106, and Physics Department, KAIST, 305-701 Daejon, Republic of Korea

Received August 13, 2002

ABSTRACT: We theoretically study the polarizability and the interactions of neutral complexes consisting of a semiflexible polyelectrolyte adsorbed onto an oppositely charged spherical colloid. In the systems we studied, the bending energy of the chain is small compared to the Coulomb energy and the chains are always adsorbed on the colloid. We observe that the polarizability is large for short chains and small electrical fields and shows a nonmonotonic behavior with the chain length at fixed charge density. The polarizability has a maximum for a chain length equal to half of the circumference of the colloid. For long chains, we recover the polarizability of a classical conducting sphere. For short chains, the existence of a permanent dipole moment of the complexes leads to a van der Waals-type long-range attraction between them. This attractive interaction vanishes for long chains (i.e., larger than the colloidal size), where the permanent dipole moment is negligible. For short distances the complexes interact with a deep short-ranged attraction which is due to energetic bridging for short chains and entropic bridging for long chains. Exceeding a critical chain length eventually leads to a pure repulsion. This shows that the stabilization of colloidal suspensions by polyelectrolyte adsorption is strongly dependent on the chain size relative to the colloidal size: for long chains the suspensions are always stable (only repulsive forces between the particles), while for midsized and short chains there is attraction between the complexes and a salting-out can occur.

I. Introduction

Polyelectrolyte− (PE−) colloid complexes have recently motivated a great amount of computational and analytical work.[1−21] The reason for this is not only the interesting behavior seen in such systems, but also their potential applications. For instance, some water-soluble paints are formed by PE−colloid complexes, in which a colloidal suspension is stabilized by adsorbed charged polymers. A better understanding of these complexes can give hints on how to avoid the precipitation of the particles from the suspension. Another example is the DNA−histone complex,[1−3] whose behavior is thought to be one of the crucial factors in the packing of DNA in living cells.[4]

Most of the previous work on PE−colloid complexes looked essentially at the structure and complexation behavior of the aggregates, e.g., of one PE and one macroion,[1,5−17] one PE and many macroions,[12,14,15,18] one macroion and many PEs,[6] or the effect of overcharging of the macroion.[8,10,17−19] While some works discuss the interactions between two macroions in the presence of either one or more than two short PE chains,[18,20,21] we concentrate here on the complex formed by one spherical colloid and one PE as a whole and look at its polarizability, as well as the effective interaction[22] between two isolated complexes. To do this we perform Monte Carlo (MC) computer simulations of one and two neutral symmetric PE−colloid complexes, i.e., systems where the charge of the PE exactly neutralizes the charge of the colloidal particle. We focus on the case where the bending energy is small compared to the energy of Coulomb coupling; i.e., the chain is always completely adsorbed on the macroion.

While the results we will show are, strictly speaking, only valid in the limit of low density of complexes and zero salt concentration, we expect these to remain qualitatively correct under more realistic conditions. This conclusion is supported by a qualitative analysis of the effect of salt: as we will show, the results obtained for the salt-free system are essentially the same if salt is taken into account in the simulations through a Debye−Hückel interaction. Also, while both the polarizability and the interaction between complexes is very much influenced by the "microscopics" (i.e., by the structure of the chain), we will show that most of the computer simulation results can be understood using fairly simple principles.

In our calculations, we focus on the case where the complexes are neutral or weakly charged. We show that a solution consisting of these neutral complexes are very likely to be stable if the adsorbed chains are long compared to the circumference of the sphere which leads to an effective repulsion between such complexes. Our calculations concerning the polarizability are not meant to apply directly to experiments in the presence of an external electrical field[23] but more toward understanding the polarizability in the context of interactions between nucleosome-like complexes which may be governed by electrostatic forces including induced dipolar interactions.

* Corresponding author; E-mail address: joachim@thphy.uni-duesseldorf.de; URL: www2.thphy.uni-duesseldorf.de/~joachim.
† Heinrich-Heine-Universität Düsseldorf.
‡ Materials Research Laboratory, University of California, Santa Barbara.
§ Kavli Institute for Theoretical Physics, University of California, Santa Barbara.
|| KAIST.

10.1021/ma021322l CCC: $25.00
Published on Web 02/14/2003

The paper is organized as follows. In section II, we describe the model used and the computer simulation details. In section III ,we present the simulation results for the dipole moment in an external electrical field of one PE−colloid complex and suggest analytical expressions for the polarizability for all chain lengths. Section IV deals with the interaction of two of these complexes for different distances and chain lengths. We describe how the force is calculated and the results are discussed. We provide analytical results for the force for short chain lengths and long distances. Finally in section V we make some final remarks.

II. The Simulation Model

We performed monomer-resolved Monte Carlo (MC) simulations using the model of Kremer et al. for single polyelectrolyte (PE) chains.[24−26] The polyelectrolyte chains are modeled as bead−spring chains of N Lennard-Jones (LJ) particles. This method was first applied to neutral linear polymers and to a single star polymer[25,26] later also for neutral[27,28] and charged stars polymer systems.[29,30] For good solvent conditions, a shifted LJ potential is used to describe the purely repulsive excluded volume interaction between all N monomers:

$$V_{\mathrm{LJ}}(r) = \begin{cases} 4\epsilon_{\mathrm{LJ}}\left[\left(\frac{\sigma}{r}\right)^{12} - \left(\frac{S}{r}\right)^{6} + \frac{1}{4}\right] & \text{for } r \le 2^{1/6}\sigma \\ 0 & \text{for } r > 2^{1/6}\sigma \end{cases} \quad (1)$$

Here, r is the distance of the interacting beads, σ is the microscopic length scale of the beads, and ϵ_{LJ} sets the energy scale. We will from now on rescale all lengths with σ according to

$$\tilde{r} = \frac{r}{\sigma} \quad (2)$$

In accordance with previous work,[27,29,30] we have chosen for the temperature $T = 1.2\epsilon_{\mathrm{LJ}}/k_{\mathrm{B}}$, where k_{B} is the Boltzmann constant.

The connectivity of the bonded monomers is assured by a finite extension nonlinear elastic (FENE) potential acting between neighboring beads

$$V_{\mathrm{F}}(r) = \begin{cases} -\frac{1}{2}k_{\mathrm{F}}\left(\frac{r_{\mathrm{m}}}{\sigma}\right)^{2} \ln\left[1 - \left(\frac{r}{r_{\mathrm{m}}}\right)^{2}\right] & \text{for } r \le r_{\mathrm{m}} \\ \infty & \text{for } r > r_{\mathrm{m}} \end{cases} \quad (3)$$

where k_{F} denotes the spring constant and is set to $k_{\mathrm{F}} = 7.0\epsilon_{\mathrm{LJ}}$. This interaction diverges at $r = r_{\mathrm{m}}$, which determines the maximal relative displacement of two neighboring beads. The energy ϵ_{LJ} is the same as in eq 1, whereas for the length scale r_{m} we have chosen the value $\tilde{r}_{\mathrm{m}} = 2.0$.

Finally, the full Coulomb interaction $V_{\mathrm{C}}(r)$ between all charged monomers has to be taken into account

$$V_{\mathrm{C}}(r_{ij}, Z_i, Z_j) = \frac{Z_i Z_j e^2}{4\pi\epsilon_0\epsilon_{\mathrm{r}} r_{ij}} \equiv k_{\mathrm{B}}T\ell_{\mathrm{B}}\frac{z^2}{r_{ij}} \quad (4)$$

where Z_i and Z_j are the number of elementary charges of the interacting particles i and j, e is the elementary charge, and r_{ij} is the distance between the particles. In our polymer model, every monomer has charge valence z, meaning that the total charge valence of one PE is simply given by $Z \equiv Nz$. The Bjerrum length ℓ_{B} is defined as the length at which the electrostatic energy equals the thermal energy, viz.

$$\ell_{\mathrm{B}} = \frac{e^2}{4\pi\epsilon_0\epsilon_{\mathrm{r}}k_{\mathrm{B}}T} \quad (5)$$

where $\epsilon_0\epsilon_r$ is the permittivity of the solvent. For water in room-temperature one obtains $\ell_{\mathrm{B}} = 7.1$ Å. The solvent is only taken into account via the dielectric constant $\epsilon_0\epsilon_r$. In our simulations, the Bjerrum length is fixed to $\tilde{\ell}_{\mathrm{B}} = 3.0$, which is a realistic value for typical polyelectrolytes, such as the hydrophobic sodium poly(styrene-*co*-styrenesulfonate) (NaPSS) or the hydrophilic poly(acrylamide-*co*-sodium-2-acrylamido-2-methylpropanesulfonate).[31]

The interaction between one PE and a spherical macroion of radius R_0 is modeled as follows: a monomer in distance r from the center of the colloid has a repulsive interaction $V_{\mathrm{LJ}}^{\mathrm{m}}(r)$ of the truncated and shifted Lennard-Jones type

$$V_{\mathrm{LJ}}^{\mathrm{m}}(r) = \begin{cases} \infty & \text{for } r \le R_0 \\ V_{\mathrm{LJ}}(r - R_0) & \text{for } r > R_0 \end{cases} \quad (6)$$

and an attractive Coulomb interaction $V_{\mathrm{C}}(r, -Z, z)$, i.e., electrostatic interaction between a monomer of charge valence z and an opposite charge at the center of the macroion with valence $Z = Nz$, which exactly neutralize the charge of the polyelectrolyte. Naturally, the repulsive interaction between two macroions each with charge valence Z in distance r is given by $V_{\mathrm{C}}(r, Z, Z)$. At a later stage we will include the effect of added salt by using a Debye−Hückel (screened) interaction, via

$$V_{\mathrm{DH}}(r_{ij}, Z_i, Z_j) = \ell_{\mathrm{B}}\frac{Z_i Z_j \exp[-\kappa(r_{ij} - R_i - R_j)]}{\beta r_{ij} \quad (1 + \kappa R_i)(1 + \kappa R_j)} \quad (7)$$

where R_i and R_j are the hard core radii of the two interacting particles, in particular R_0 for the macroions and zero for the monomers and κ is the inverse screening length.[32] The inverse temperature is denoted by $\beta = 1/k_{\mathrm{B}}T$. κ is related to the z-valent salt molar concentration c_{s} (mol per liter) via

$$c_{\mathrm{s}} = \kappa^2/8\pi N_{\mathrm{A}}\ell_{\mathrm{B}}z^2 \quad (8)$$

where N_{A} is Avogadro's number. We stress the fact that in the absence of salt, the system contains no small counterions: the chain and colloidal particle exactly cancel each others charge.

In this work, we focus our attention on the case where the bending energy of the chain is small compared to the Coulomb energy of the complex. A good estimate of the bending energy of a chain with persistence length l_{p} (isolated chain) and contour length l wrapped around a macroion to build a complex with radius R is given by

$$E_{\mathrm{bend}} = k_{\mathrm{B}}T\frac{l_{\mathrm{p}}l}{2R^2} \quad (9)$$

This should be small compared to the Coulomb energy, which yields

$$2Z^2\frac{\ell_{\mathrm{B}}R}{l_{\mathrm{p}}l} \gg 1 \quad (10)$$

as the condition for a complete adsorption of the chain. We measured the persistence length of an isolated chain by calculating the bond vector correlations in dependence of the contour distance between the bonds and determining the typical decay length. We find a linear dependence $l_p \approx l/2$ for a wide range of contour lengths if no intrinsic stiffness is applied. Inserting this scaling relation in eq 10 and using $Z \approx \tilde{l}z$ gives us a simple estimate for the wrapping state for chains with no intrinsic stiffness

$$4z^2\tilde{l}_B\tilde{R} \gg 1 \tag{11}$$

Another limit where desorption can take place if the Coulomb coupling is small compared to the thermal fluctuations; e.g., the macroion is very big compared to the chain size. There is a complete adsorption of the chain onto the colloid if the electrostatic attraction is larger than the thermal fluctuations

$$Z^2\frac{\ell_B}{R} \gg 1 \tag{12}$$

Strictly speaking, the adsorbed state is metastable: if the colloid and the finite chain are initially put far apart from each other, they interact essentially like two pointlike charges. It is well-known that the $1/r$ potential between two charges is not enough to bind them together; i.e., the Coulomb potential between two point charges is not enough to compensate for the loss of entropy through binding (cf. Manning condensation.[33]) However, if the particles are put enough close to each other, the system needs a very long time before the unbound stable state is reached. To see this, let us assume that two oppositely charged particles are confined to a "spherical" box of radius L. The probability of finding them at distance r from each other is given by

$$\mathcal{P}(r) = \frac{\exp\{Z^2\ell_B/r\}}{\mathcal{Z}} \tag{13}$$

where $\mathcal{Z} = \int_R^L \mathrm{d}r\ \mathcal{P}(r)$ and R is the contact distance between the charges. The ratio between the probability of finding the particles at $r' = r + \ell_B$ and at r is then given by

$$R_{\mathcal{P}} = \exp\{-Z^2\ell_B^2/(r(r+\ell_B))\} \tag{14}$$

For $r = \ell_B$ and $Z = 10$, this corresponds to $R_{\mathcal{P}} \sim 2 \times 10^{-22}$. In other words, if the two charges are initially put ℓ_B apart, the probability of finding them at $2\ell_B$ apart is much smaller than to find them at ℓ_B. Note that $R_{\mathcal{P}}$ increases with r: if the particles are initially put very far apart from each other (e.g. r/ℓ_B on the order of Z), the system will flow to the stable state much faster, since the ratio $R_{\mathcal{P}}$ become of order unity. In our simulations, and in agreement with previous works, the PE has always stayed at the close vicinity of the colloidal particle, since the parameters are chosen such that eqs 10 and 12 are always satisfied.

Increasing chain stiffness has great influence on polarizability and interaction of these complexes. Some possible effects will be discussed briefly by introducing a simple harmonic coupling between the bonds of one PE

$$V_{\mathrm{bond}} = \sum_{i=2}^{N-1k} k_{\mathrm{ang}}(\alpha_i - \alpha_0)^2 \tag{15}$$

where α_i is the angle formed between the connecting vectors of bonds i and $i-1$ and the bonds i and $i+1$. We choose an equilibrium angle $\alpha_0 = \pi$ and examine the effects of increasing chain stiffness by enhancing the bonding constant k_{ang}. Unless if explicitly mentioned, k_{ang} is always chosen to be zero.

We applied the standard MC Metropolis algorithm[34] where one MC step consists of a trial move of every monomer. The macroions were kept fixed. The acceptance rate for one MC sweep was approximately 50%. For faster equilibration and better statistics we introduced full chain moves where the whole PE is rotated around the closest macroion. Details describing these methods can be found in.[35,36] Our systems were simulated without any cell in an infinitely wide space where the full accurate Coulomb interaction without an cutoff is taken into account. We observed that only at low Coulomb coupling or large intrinsic stiffness the thermal fluctuations lead to an entropic uncoupling of chain and colloid. After a long equilibration time (typically of 1.5×10^5 to 2×10^5 MC steps), the different observables were averaged over runs with 10^6 to 10^7 MC steps.

III. Polarizability of a Single Complex

In this section we study the polarizability of a single complex consisting of one PE chain with contour length l and linear charge density $\tau = Ze/l$ ($Z = Nz$ and e is the elementary charge unit) which is adsorbed onto a spherical colloid with radius R_0 and charge valence Z. To calculate the contour length in the simulation, we measure the mean distance between neighboring monomers: for a monomer charge $z = 1$ we obtain $l \approx N\sigma$ and for $z = 2$ we obtain $l \approx 1.3N\sigma$; i.e., $\tau\sigma = \tilde{\tau} = 1$ for $z = 1$, and $\tilde{\tau} = 1.54$ for $z = 2$. In what follows, we will extensively use as a parameter the ratio between the PE length and the *effective* diameter of the complex ($2R$)

$$x \equiv \frac{l}{2R} \tag{16}$$

For $x = \pi$ the chain length is equal to the circumference of the complex. For a chain much thinner than the colloid radius and at low temperatures, the effective radius R should be given by $R \approx R_0$. However, since in our simulations the monomers have a size that is comparable to the colloidal particle, this effective radius is approximately $R \approx R_0 + \sigma$, with some dependence on the number of monomers in a chain and on the charge of each monomer, as can be seen in Figure 1. In this figure, we show the density profile $\rho(r)$ of the monomers surrounding a colloid with radius $\tilde{R}_0 = 5$ for chains with different number of monomers N and different monomer charges $z = 1, 2$. As one would expect, a higher Coulomb coupling between the PE and the colloid (through a higher total charge in the PE) leads to a reduction of the effective radius of the complex, here assumed to be at the maximum of the monomer distribution. Simulation snapshots are shown in Figure 2 for systems with different numbers of monomers and no external field. As already mentioned, the dependence of R on the parameters of the PE is so weak that it can be assumed for all practical purposes to be a constant for a wide range of chain lengths. In the following, we will choose

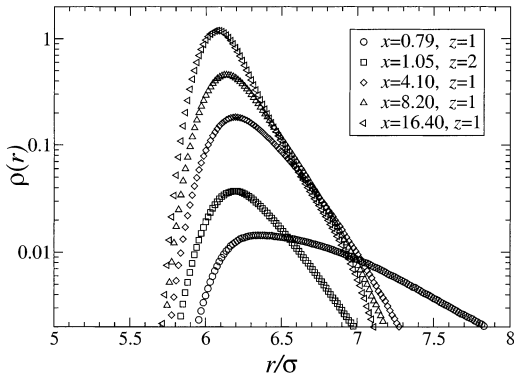

Figure 1. Density profile of the monomers of one chain adsorbed to a spherical colloid with radius $\tilde{R}_0 = 5$ for different chain length x and different number of charges per monomer z plotted vs the distance $\tilde{r}$ to the center of the colloid. With increasing x and z, the monomers move closer to the center, and the effective complex radius R decreases. See Figure 2 for simulation snapshots of one isolated complex.

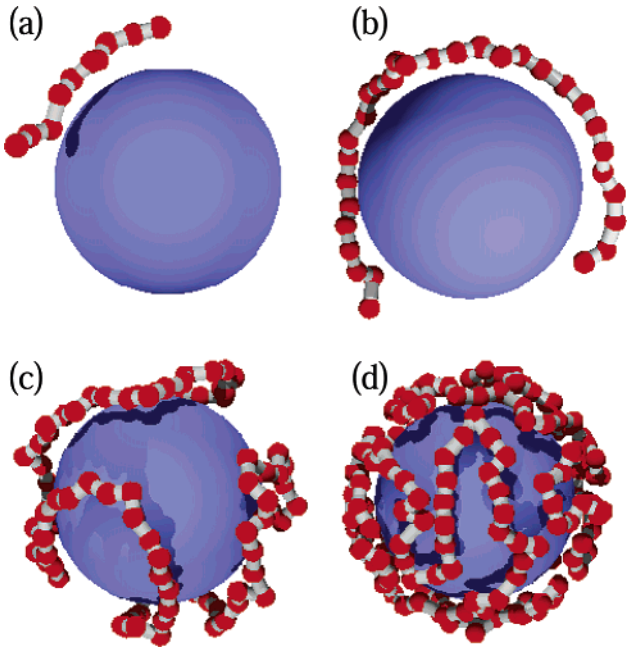

Figure 2. Computer simulation snapshots of a PE adsorbed to a spherical colloid with radius $\tilde{R}_0 = 5$ for (a) $x = 0.79$, (b) $x = 2.78$, (c) $x = 8.20$, and (d) $x = 16.40$. The number of elementary charges per monomer is $z = 1$. The monomers are rendered as dark spheres with diameter σ.

Table 1. Parameters of the Simulated System for $z = 1$ and $\tilde{R}_0 = 5$

N	10	15	20	25	30	35	40	50	100	200	300
$\tilde{R}$	6.3	6.3	6.3	6.3	6.3	6.3	6.1	6.1	6.1	6.1	6.1
x	0.79	1.19	1.59	1.98	2.38	2.79	3.27	4.10	8.20	16.40	24.60

[a] We simulated chains with different monomer numbers N and chose a fixed complex radius R according to the density profiles, see Figure 1. $x = l/2R$ are the corresponding chain lengths, while $l = N\sigma$ for $z = 1$.

$\tilde{R} = 6.3$ for short chains $x < \pi$ and $\tilde{R} = 6.1$ for long chains $x > \pi$ as effective complex radius, for a fixed colloid radius $\tilde{R}_0 = 5.0$ and $z = 1$. See Table 1 for a summary of the relation between complex radius, monomer number, and chain length for the simulated system with $z = 1$. The lengths for $z = 2$ can be calculated accordingly; here, we used $R = 6.2$ for $x < \pi$ and $R = 6.0$ for $x > \pi$. The colloid valence is simply given by $Z = Nz$. We checked that all forthcoming results obtained from the simulations are independent of above particularly chosen radius of the colloid. All theoretical results in this and the following section should hold generally for all colloid sizes.

We start our analysis with chains which are short compared to the size of the colloid, viz. $x < \pi$. In this regime the PE−colloid complex has always a nonvanishing instantaneous dipole moment, since the center of charge of the chain cannot coincide with the center of the colloid. We define the dipole moment $\vec{P}$ of the complex as

$$\vec{P} = \frac{Ze}{N}\sum_{i=1}^{N}(\vec{r}_i - \vec{R}_c) \tag{17}$$

where $\vec{R}_c$ is the vector pointing to the center of the colloid and $\vec{r}_i$ is the position of monomer i. Notice that, with this definition, the magnitude of $\vec{P}$ is given by Ze times the distance between the center of the colloid and the center of charge of the PE chain. It is easy to show that the mean dipole moment of a thermally fluctuating rigid dipole with length d and charge Ze in an electrical field E is

$$P = Zed\left(\coth(\beta ZedE) - \frac{1}{\beta ZedE}\right) \tag{18}$$

where P is the magnitude of $\vec{P}$ and $\beta \equiv 1/k_BT$. Introducing the rescaled dimensionless dipole moment

$$P^* = \frac{P}{\sigma e} \tag{19}$$

and electric field

$$E^* = \beta\sigma eE \tag{20}$$

one can rewrite eq 18 as

$$P^* = Z\tilde{d}\left(\coth(Z\tilde{d}E^*) - \frac{1}{Z\tilde{d}E^*}\right) \tag{21}$$

where $\tilde{d} = d/\sigma$. For low temperatures or strong electrical fields $Z\tilde{d}E^* \gg 1$, the mean dipole moment saturates to $P^* = Z\tilde{d}$, while for small fields $Z\tilde{d}E^* \ll 1$ and we recover the well-known result

$$P^* = \frac{Z^2\tilde{d}^2}{3}E^* \tag{22}$$

For the case of a chain adsorbed onto a spherical colloid, the center of charge of the chain is on average somewhere between the center of the colloid and its surface. Assuming that the chain can be approximately described by a circular arc fluctuating on the surface of the colloid (see, e.g., Figure 2b), the distance between the center of the colloid and the center of charge of the chain is given by

$$\tilde{d} = \tilde{R}\frac{\sin(x)}{x} \tag{23}$$

where $\tilde{R} = R/\sigma$. Our model is assumed to work for chains shorter than the circumference of the sphere; i.e., eq 23 holds for $0 < x < \pi$.

In Figure 3, we compare the dipole moment of a complex in an external field for various chain lengths and $z = 1$ as a function of the external field from computer simulations and from eq 21. Note that $\tilde{R}_0 =$

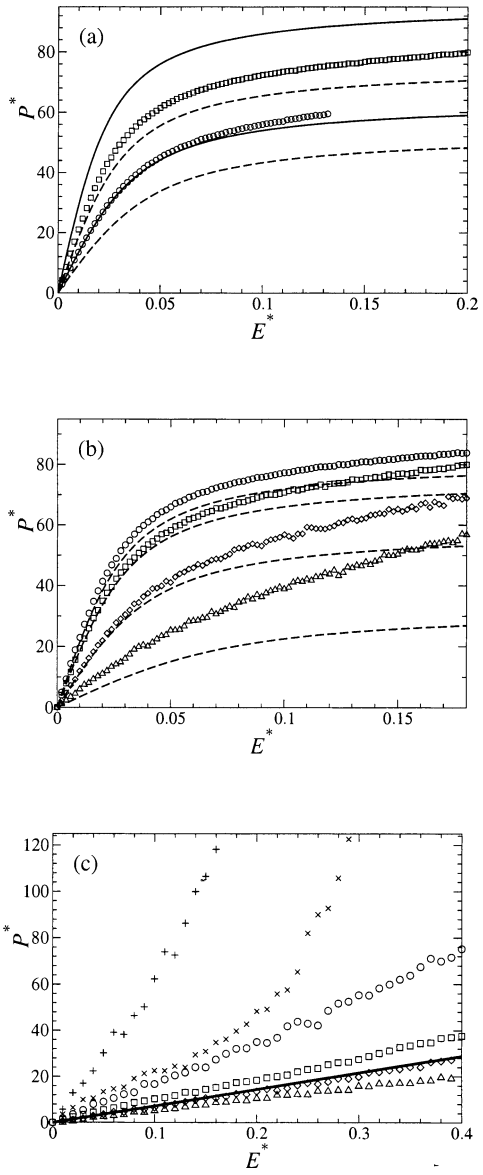

Figure 3. Dimensionless dipole moment $P^* = P/\sigma e$ of one PE−colloid complex vs the dimensionless external electrical field $E^* = \beta\sigma eE$ for different chain lengths, $z = 1$ and a colloidal radius $\tilde{R}_0 = 5$. Symbols are computer simulation results, lines are theoretical results. Plot a shows the scaled chain lengths $x = 0.79$ (circles) and $x = 1.19$ (squares). The dipole moment increases with x. Lines are the theoretical results, eq 21, using $\tilde{d} = \tilde{R}$ (solid) or the effective dipole length $\tilde{d} = \tilde{R}\sin(x)/x$ (long dashed). Plot b shows the results for $x = 1.59$ (circles), $x = 1.98$ (squares), $x = 2.38$ (diamonds), and $x = 2.78$ (triangles). Note that the dipole moment now decreases with increasing x. The long dashed lines is theory as used in part a. Plot c shows the results for $x = 4.10$ (circles), $x = 8.20$ (squares), $x = 16.40$ (diamonds), and $x = 24.60$ (triangles). The solid line is the dipole moment of a conducting sphere with radius $\tilde{R}_{cs} = 6.1$ according to $P^* = \alpha_{cs}E^*$, where α_{cs} is given by eq 26. In (c) we also show the effect of increasing chain stiffness for $x = 4.10$. The harmonic coupling is quantified by $\beta k_{ang} = 4.0$ (crosses) and $\beta k_{ang} = 5.0$ (plusses).

5, and the effective radius is assumed to be $\tilde{R} = 6.3$ for $x \lesssim \pi$. For the theoretical effective dipole length d, we use the result from eq 23 when $0 \lesssim x \lesssim \pi$ and 10 is satisfied. If eq 10 is not fulfilled, the chain is essentially a straight rod that touches the sphere—in this case, the effective length of the dipole is simply given by R. On the other hand, for $x \gtrsim \pi$ the chain cannot be approximated by a two-dimensional circle and eq 21 breaks down.

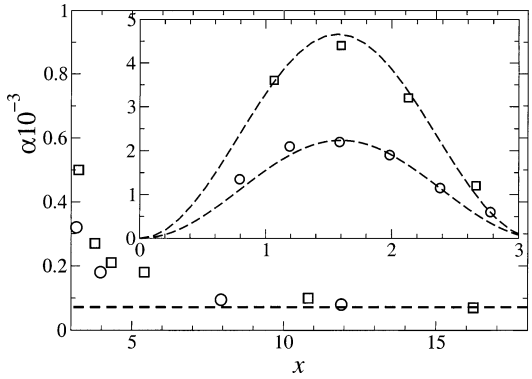

Figure 4. Dimensionless polarizability α vs the scaled chain length x at small applied fields. The symbols denote the simulation, the dashed lines are the theoretical results from eq 25 (inset) and eq 26 for charges per monomer $z = 1$ (circles) and $z = 2$ (squares). The colloid radius is $\tilde{R}_0 = 5$.

The polarizability α of the complex is defined as the slope of its dipole moment as a function of the electric field

$$\alpha = \frac{dP^*}{dE^*} \tag{24}$$

The behavior of α is shown in Figure 4: in the regime of small electric fields, the polarizability is constant, here we are in the linear response regime, see eq 22.

In the regime where the interaction energy between the dipole and the applied field largely exceeds the thermal energy ($Z\tilde{d}E^* \gg 1$) the polarizability becomes very small; this latter behavior is not surprising, since in this regime the dipole is essentially pointing toward the field, and thermal fluctuations which tend to destroy this alignment at small fields become unimportant. In our simulations we never really reach the point where the polarizability becomes zero since at some point the field is strong enough to induce the unbinding of the chain from the colloidal particle. Figure 3a shows the dipole moment for two short chains, viz. $x = 0.79$ and $x = 1.19$. Notice that the system with former value of x is very well described by P with $d = R$, while the latter tends to approach the dipole moment which uses d given by eq 23. The reason for this is the fact that in the system with smaller x the polyelectrolyte has a bending energy on the order of the Coulomb energy of the complex, see eq 10, and the system behaves more like a rigid rod in contact with a sphere than as a circular arc, as described by eq 23. The curve for $x = 0.79$ in Figure 3a stops abruptly since the critical field for the desorption is reached.

Longer chains lead to a decrease of the polarizability at small fields as can be seen in Figure 3b, where we plot $x = 1.59$, 1.98, 2.38, and 2.78. This effect is a result of the dislocation of the center of charge of the chain to a position that is closer to the center of the colloid, according to eq 23. Note that complexes with medium-sized chains tend to approximately exhibit dipole moment of a circular arc on a sphere. However, complexes with long chains, $x \gtrsim \pi$ tend to have a linear response to a wider range of the applied field (see Figure 3, parts b and c), which is a consequence of the fact that larger chains have more charge at fixed charge density, and so the fields needed to deviate from a linear law are larger; also, the fact that longer chains have more possible conformations leads to a qualitative change in

the response of the complex, and a simple model as the one used above is no longer valid.

Let us have a closer look at the polarizability for small fields and short chains. Inserting eq 23 into eq 22, one obtains, for small fields, the dimensionless polarizability of the complex as a function of the PE chain length and charge density

$$\alpha = \frac{4\tilde{\tau}^2\tilde{R}^4}{3}\sin^2(x) \qquad (25)$$

where the linear charge density τ has been rescaled such that $\tilde{\tau} = \sigma\tau$. For a fixed τ, this polarizability shows a maximum at $x = \pi/2$ for a chain with length equal to half the circumference of the colloid and vanishes for $x = \pi$, when a chain has a full circumference. Indeed, this behavior predicted by theory is very close to in the computer simulation results in the inset of Figure 4, where we plot α for small fields for a colloid with fixed radius $\tilde{R}_0 = 5$ and $\tilde{R} = 6.3$ and monomer charges $z = 1$ and $z = 2$.

In the cases where the complex contains a long chain $x \gtrsim \pi$, the polarizability eq 25 loses its validity. Note that in this case, the chain is wrapped around the sphere more than one time and one expects a small or vanishing dipole moment. Because the monomers tend to distribute themselves on average more or less homogeneously throughout the surface of the sphere, one could expect the response of the PE−colloid complex to electric fields to become similar to the response of a neutral conducting sphere, which has a dimensionless polarizability given by (see., e.g., ref 37)

$$\alpha_{cs} = \frac{\tilde{R}_{cs}^{\ 3}}{\tilde{\ell}_B} \qquad (26)$$

where R_{cs} is the radius of the sphere and $\tilde{\ell}_B = \ell_B/\sigma$. Not surprisingly, in the limit of very large chains $x \gg \pi$ this latter result is recovered, as shown in Figure 4. For this comparison we have chosen $\tilde{R}_{cs} = 6.1$ for the effective sphere radius. Note that the simulation results for long chains are independent of the linear charge density in agreement with eq 26.

Let us now discuss possible effects of an increasing intrinsic stiffness of the chain. For short chains, we observe an increasing polarizability if the harmonic coupling is strong enough to decrease the curvature of the chain around the spherical macroion meaning that the bending energy reaches values on the order of the Coulomb energy.

The center of charge of the PE is not as close to the colloid center, and the effective dipole length increases. As an upper limit the maximal dipole moment is then given by eq 18 inserting $d = R$, with R being the effective complex radius. However, for the case, where the bending energy comes close to the Coulomb energy, we observe that the chain decouples easily from the colloid and no bound complex is formed.

More interesting is the behavior for long chains. For long chains with a large bending energy and no electrical field, so-called one-tail or two-tail configurations sets in.[1,5,13,15,16] Here one part of the PE is still adsorbed on the colloid while one or two rigid parts are stretched away from the macroion to lower the bending energy and so minimize the total energy. In an electrical field the one tail configuration is obviously promoted due to the strong dipolar interaction with the external field,

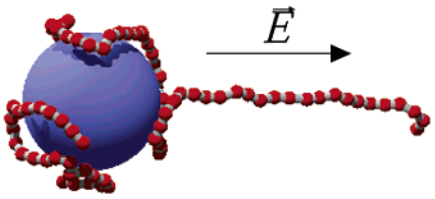

Figure 5. Simulation snapshot of a PE−colloid complex in an external electrical field E. The chain has an intrinsic stiffness due to the harmonic coupling eq 15. The bonding constant is $\beta k_{ang} = 4.0$, the number of monomers is $N = 100$, $E^* = 0.4$, $z = 1$, and $\tilde{R}_0 = 5.0$.

see Figure 5 for a simulation snapshot. We make the following observation in our simulation: if the chain is fully adsorbed on the colloid the polarizability is still given by eq 26 independent of the higher chain stiffness, only the effective complex radius increases slightly due to a less tight wrapping around the colloid. However, for a sufficiently strong chain rigidity, a small external electrical field can now pull a part of the chain in direction of the chain to lower the bending and dipole energy and a dipolar one tail configuration is formed. Two examples of the dipole moment are shown in Figure 3c for $x = 8.20$, $\beta k_{ang} = 4.0$ and $\beta k_{ang} = 5.0$. For small fields the chain is fully adsorbed and the polarizability is the same as for the $\beta k_{ang} = 0$ case. Then the increased stiffness leads to a continuous dewrapping in the one-tail configuration, and the polarizability increases dramatically due to a formed dipole. Further increasing of the electrical field lengthens the tail and eventually decoils the chain from the colloid. The longer the tail, the larger is the dipole moment and the polarizability increases with growing field until complete desorption is accomplished. A snapshot for an one-tail complex in an electrical field E is shown in Figure 5.

Finally, adding salt obviously increases the polarizability as the range and strength of the Coulomb attraction between PE and the colloid is screened and the effective complex radius grows. We take the presence of salt into account by using a Debye−Hückel potential between the monomers (and ignoring any polarizability due to the salt), going up to a salt concentration of $c_s \approx 1.5$ M. We observe that eq 25 for short chains and eq 26 for long chains still hold as long a stable complex is formed but with a slightly larger effective radius R or R_{cs}, respectively.

IV. Effective Interaction between Two Complexes

We now turn to the interaction between two complexes at distance r. The effective force acting on the center of one colloid in the simulation is calculated as follows: consider two spherical colloids with radius R_0 and center-to-center distance r, which means that they have a surface-to-surface distance of $s = r - 2R_0$. The energy of one colloid in the presence of one monomer at distance r^m is the sum of Coulomb attraction and short-ranged LJ-repulsion

$$V_{mon}(r^m) = V_C(r^m, -Z, z) + V_{LJ}^m(r^m) \qquad (27)$$

After a sufficiently long equilibration time, the force F_m of all monomers acting on one of the colloids is measured by performing the statistical average

$$F^{\mathrm{m}}(r) = \langle \sum_{i=1}^{M}\sum_{j=1}^{N} \nabla_{\mathrm{r}} V_{\mathrm{mon}}(r_{ij}^{\mathrm{m}}) \rangle \tag{28}$$

where the sum in i goes over all M PE chains and the sum in j considers all N monomers of each chain. r_{ij}^{m} is the distance of monomer j from the ith PE chain to the center of the considered colloid. The brackets in eq 28 denote ensemble statistical average. We obtain the total force between the colloids in distance r by adding the direct repulsive Coulomb force between the colloidal particles, viz. $Z^2e^2/4\pi\epsilon_0\epsilon_r r^2$. The total force can be then divided into two contributions

$$F(r) = F_{\mathrm{C}}(r) + F_{\mathrm{LJ}}(r) \tag{29}$$

where

$$F_{\mathrm{C}}(r) = \frac{Z^2e^2}{4\pi\epsilon r^2} + \langle \sum_{i=1}^{M}\sum_{j=1}^{N} \nabla_{\mathrm{r}} V_{\mathrm{C}}(r_{ij}^{\mathrm{m}}, Z, z) \rangle \tag{30}$$

is the Coulomb force due to the electrostatic attraction of all monomers and the electrostatic repulsion of the second colloid and

$$F_{\mathrm{LJ}}(r) = \langle \sum_{i=1}^{M}\sum_{j=1}^{N} \nabla_{\mathrm{r}} V_{\mathrm{LJ}}(r_{ij}^{\mathrm{m}}) \rangle \tag{31}$$

resulting from the excluded volume interaction of the monomers through the aforementioned Lennard-Jones potential. Since this force is essentially a hard-core exclusion force, one can consider this as describing the interaction due to gain and loss of entropy. For this reason, we call it entropic force.

On the basis of the previous discussion on the polarizability of a single complex, one can essentially expect two distinct regimes for the interaction between two equal symmetric complexes, viz. when the chains are short and when the chains are long. Figure 6 summarizes our results, where the dimensionless force $F^* = \beta\sigma F$ is plotted for systematical increase of x and $z = 1$ as a function of s, the surface-to-surface distance. Negative forces mean attraction while positive forces mean repulsion. See Figure 7 for some typical simulation snapshots. Notice that for short chains, a long-range attractive tail is present. This is consistent, as we will demonstrate, with a dipolar interaction between the complexes. For longer chains, this long-range tail disappears, and only a strong short-range attraction (also present for shorter chains) survives. In the limit of very long chains, only a repulsive steric interaction is present. We discuss these results in more detail in the following.

A. Short Chains. In the previous section, we showed that the complexes with short chains respond like permanent dipoles to electric fields. When interacting with each other, it is reasonable to expect that in such case a dipole−dipole interaction shows up, at least at large separations between complexes. One way of estimating this long-range tail is by looking at the interaction between two fluctuating permanent dipoles $P = Zed$ with length d as given by eq 23 expressed through the so-called Keesom energy[38]

$$\beta v(r) = \frac{1}{3}\frac{Z^4 \tilde{l}_{\mathrm{B}}{}^2 \tilde{d}^4}{\tilde{r}^6} \tag{32}$$

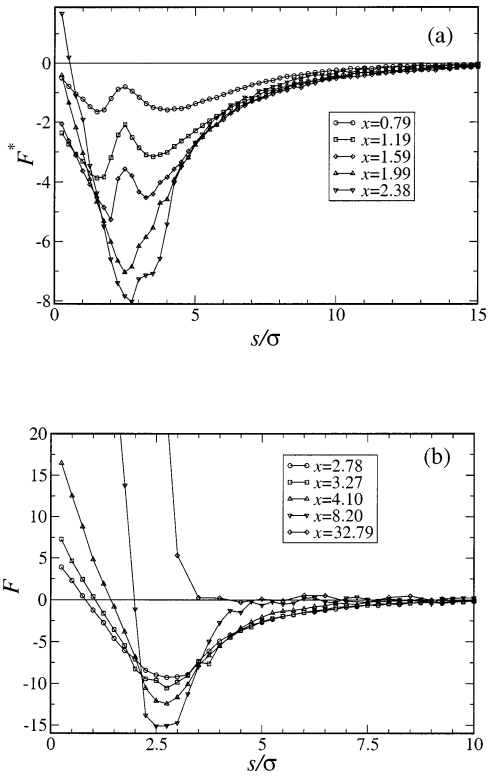

Figure 6. Simulation results of the dimensionless force $F^* = \beta\sigma F$ between two PE−colloid complexes vs the surface−surface distance $\tilde{s}$ for different chain lengths x and $z = 1$. The colloid radius is $\tilde{R}_0 = 5.0$. Lines are guide to the eye. Plot a: short chains $x \lesssim \pi$. Plot b: long chains $x \gtrsim \pi$.

After some algebra, one obtains for the interaction energy between two PE−colloid complexes with $0 \lesssim x \lesssim \pi$

$$\beta v(r) = -\frac{16\tilde{l}_{\mathrm{B}}{}^2\tilde{\tau}^4\tilde{R}^8}{3\tilde{r}^6}\sin^4(x) \tag{33}$$

where r is the distance between the dipole and the polarizable object. Accordingly, the attractive force acting on the polarizable object is

$$F^*(r) = -\frac{32\tilde{l}_{\mathrm{B}}{}^2\tilde{\tau}^4\tilde{R}^8}{\tilde{r}^7}\sin^4(x) \tag{34}$$

We easily see that the electrostatic interaction has a maximum of strength for a length $x = \pi/2$ according to the behavior of the polarizability of one isolated maximum. Another remarkable feature is the strong dependence on the complex radius which goes with the eighth power for a fixed x. A comparison of expression 34 with the long distance tail of the force between the complexes is done in Figure 8 for different chain lengths and charge densities, leading as expected to a nice agreement. As theoretically predicted the simulations show a maximal dipole interaction for a length $x \approx \pi/2$.

To obtain some insight into the conformational properties of the interacting complexes we introduce the order parameter

$$\phi = \frac{\vec{P}_1\vec{P}_2}{|\vec{P}_1||\vec{P}_2|} \tag{35}$$

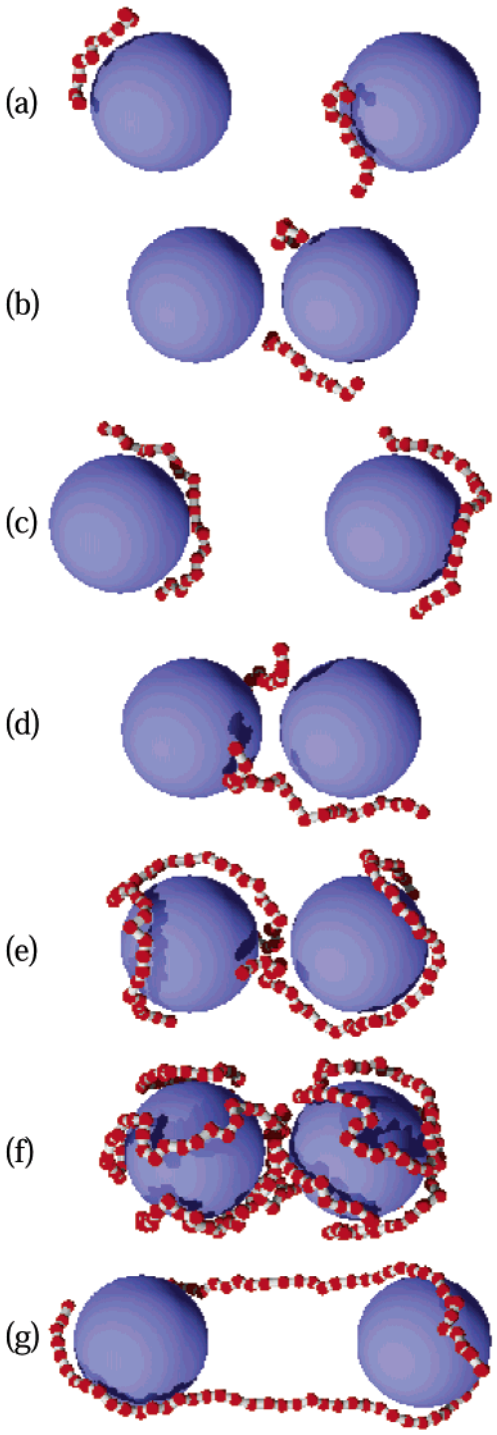

Figure 7. Snapshots of two interacting PE−colloid complexes with colloid radius $\tilde{R}_0 = 5$, $z = 1$, chain length x and surface-to-surface distance s. From top to bottom: (a) $x = 0.79$, $\tilde{s} = 8.0$; (b) $x = 0.79$, $\tilde{s} = 1.5$; (c) $x = 1.59$, $\tilde{s} = 10.0$; (d) $x = 1.59$, $\tilde{s} = 1.5$; (e) $x = 4.10$, $\tilde{s} = 2.5$; (f) $x = 8.20$, $\tilde{s} = 2.0$; (g) $x = 3.27$, $\tilde{s} = 11.25$, $\beta k_{ang} = 4.0$.

which is the normalized dot product between the two dipole moments of each complex. For a dipole−dipole interaction, $-1 \le \phi \le 1$ should be positive as both dipoles show in the same direction. Negative values of ϕ mean that the dipoles are on average pointing in opposite directions. By studying the average distance between the center of charge of the chains in our simulations, we found that every time ϕ becomes negative the monomers accumulate between the colloids,

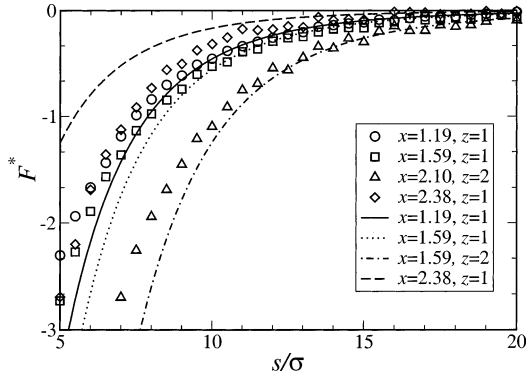

Figure 8. Interaction force between two PE−colloid complexes for long distances and short chains ($x \lesssim \pi$). The plot shows a comparison made between the analytical expression eq 34 for the dipole−dipole interaction (lines) and the computer simulation results (symbols) for colloids with size $\tilde{R}_0 = 5$ and various chains lengths x and monomer charge z.

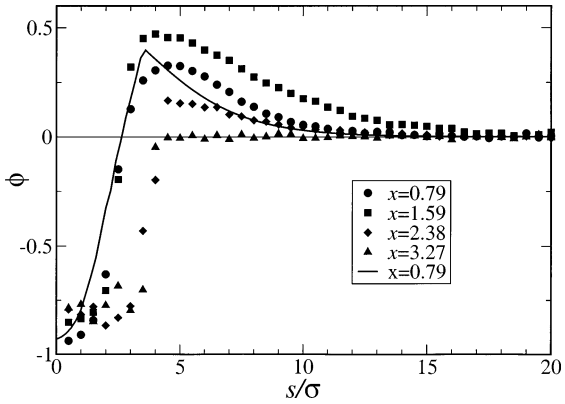

Figure 9. Simulation results (symbols) of the order parameter ϕ vs the surface-to-surface distance of two PE−colloid complexes with $\tilde{R}_0 = 5.0$, $z = 1$, and different chain lengths. The solid line is the numerical solution of the toy model sketched in Figure 10 for $x = 0.79$.

meaning that each dipole moment points in direction of the other complex in average.

Figure 9 shows ϕ as a function of separation for different chain lengths with $z = 1$ at fixed complex radius. As expected, for short chains and large distances, ϕ is positive: the dipoles of the two complexes basically point in the same direction and produce the dipole−dipole interaction as discussed above. Note that the largest values for ϕ are obtained for complexes with chains with $x = 1.59$, a value close to $x = \pi/2$ where the polarizability is maximal. Typical configurations in the dipole−dipole regime are shown in Figure 3, parts a and c, where the order parameter ϕ has positive values. A relatively sharp transition from positive to negative values of ϕ is observed for distances $\tilde{s} \approx 4$ for all values of x.

For small distances, ϕ becomes negative for all systems studied. As mentioned before, this means that the centers of charge of the chains are located somewhere between the colloids, something that turns out to be always true as $\tilde{s} \lesssim 4$. This can also be seen in snapshots for close distances of the complexes as for instance in Figure 3, parts b and d.

To obtain a better understanding of the small distance behavior of the force for complexes with short chains, Figure 3a, consider the toy model depicted in Figure 10. Here the chains are modeled as hard spheres with effective diameter a. Each sphere sticks to one colloid

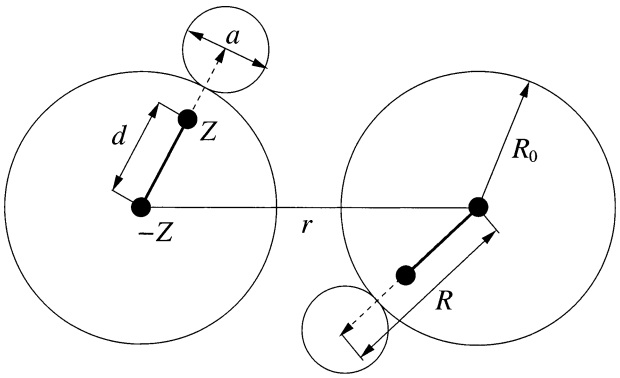

Figure 10. Schematic representation of the toy model for two PE−colloid complexes at distance r for short chain lengths ($x \lesssim \pi$). One complex behaves like a dipole with charge Z and length d (dumbbells). The short chain is modeled as a simple sphere sticking on the surface of the colloid in distance $R = R_0 + a/2$ where R_0 is the colloid radius and a is the effective diameter of the fluctuating chain.

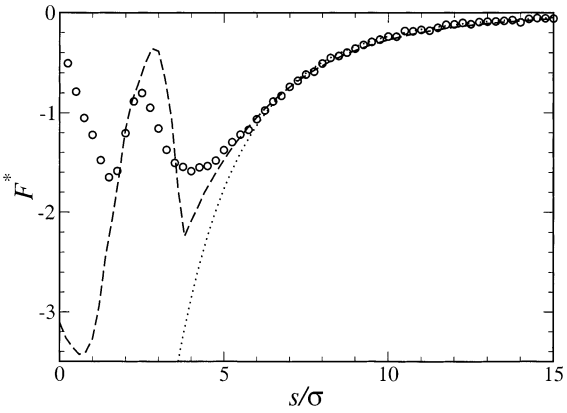

Figure 11. Interaction force between two PE−colloid complexes with a short chain $x = 0.79$ and $z = 1$. Simulation results (circles) are compared to the numerical solution of the toy model depicted in Figure 10 (dashed line) and the analytical result for the dipole−dipole interaction (dotted line).

and can only move on the surface of the macrosphere with radius R_0. One small sphere belonging to one colloid cannot penetrate into the other complex, and the center-to-center distance between the colloids is r. In this case, the effective complex radius is $R = R_0 + a/2$.

As previously shown, complexes with short chains behave like rigid dipoles with length d which is dependent on the chain contour length l. Hence, in our toy model the complex has a dipole moment in direction from the center of the colloid to the center of the small sphere with an effective length d and charge Z. For distances $r > 2(R_0 + a)$ this model shows a simple dipole−dipole attraction, whereas for smaller distances the dipole−dipole attraction is modified by the restricted number of available configurations.

One can find the force between the complexes for this toy model by numerically solving the partition sum and calculating the free energy as a function of the distance r. The results for a chain length $x = 0.79$ is plotted in Figure 11 together with the corresponding simulation data. According to the results from the previous section we use $\tilde{d} = 6.3$. We use the diameter of the small spheres a as a fit parameter, which should in any case be on the order of the monomer size. This parameter does not affect the dipole−dipole interaction, being only important when the deviations from the pure dipole−dipole interaction sets in. For $x = 0.79$ and $z = 1$, we used $\tilde{a} = 3.6$. This model leads to a qualitative agreement for the short-range behavior of the force, as depicted in Figure 11: while the scale of the force is larger for the toy model, the minima and maxima are located at approximately the right distances. In other words, this means that the behavior observed for the force at small distances and for small chains (a force with two minima) is at least partially explained by the restriction of the number of available configurations of a system that is still essentially composed by two interacting dipoles.

It is also interesting to study the behavior of the order parameter ϕ of our toy model solved for the length $x = 0.79$ and $z = 1$ also plotted in Figure 11. The qualitative behavior in dependence of the distance is quite the same as in the simulation. At $\tilde{s} \approx 4.5$ the dipole−dipole regime breaks down, and ϕ descends to negative values for closer distances s. The negative value of ϕ means that in our toy model both small spheres are located mainly between the macroions. One concludes that due to the excluded volume interaction of the small sphere/chain with the macrosphere the dipole−dipole interaction is disturbed and the spheres/chains locate themselves between the macroions, contrary to what happens in the dipole−dipole interaction regime.

B. Long Chains. Increasing the chain length, we observe a deep short-range attraction as plotted in Figure 3b which is in agreement with previous studies.[20,21,39] The depth of attraction initially grows with increasing chain length while the range of attraction shrinks. Further increasing of the chain length leads to a pure repulsion of the complexes. The attraction is essentially of entropic origin, as the comparison between the Coulomb force F_C and the entropic force F_{LJ} as defined in eqs 30 and 31 and shown in Figure 12 demonstrates: for $x = 3.27$ (large chain) the entropic force clearly dominates over the Coulombic. For distances comparable to some monomer lengths the chain is able to gain entropy by bridging the two colloids with some parts of the chain, as seen for instance in snapshots Figure 7, parts e and f. In agreement with the absence of the dipole−dipole interaction between the complexes, note that for chains with $x > \pi$, only zero or negative values of ϕ are observed: at short enough distances, the chains bridge between the colloids, otherwise the complexes basically ignore each other and no long-range force is present.

Not surprisingly, for small distances the attraction of two long chains is indistinguishable from the behavior of one chain with the combined length of the two chains, as depicted in Figure 13, where the force between two complexes with chains with $x = 4.10$ is compared with the force between to colloids in the presence of only one chain with $x = 8.20$. The force is the same for small distances $\tilde{s} < 5$ where the entropic bridging regime is found. The linear long-range attraction of the single chain system is due to an energetic bridging already observed and discussed in refs 20 and 21.

For complexes with very long chains only a pure repulsion is observable, see, e.g., $x = 32.79$ in Figure 6b. If the chain is long enough to cover the whole surface of the macroion, no bridging is possible due to the electrostatic repulsion between the approaching chain and the shell of monomers around the macroion. A simple theoretical estimate for the critical length when pure repulsion occurs is obtained by equating the available surface of the spherical complex $A = 4\pi R^2$ with

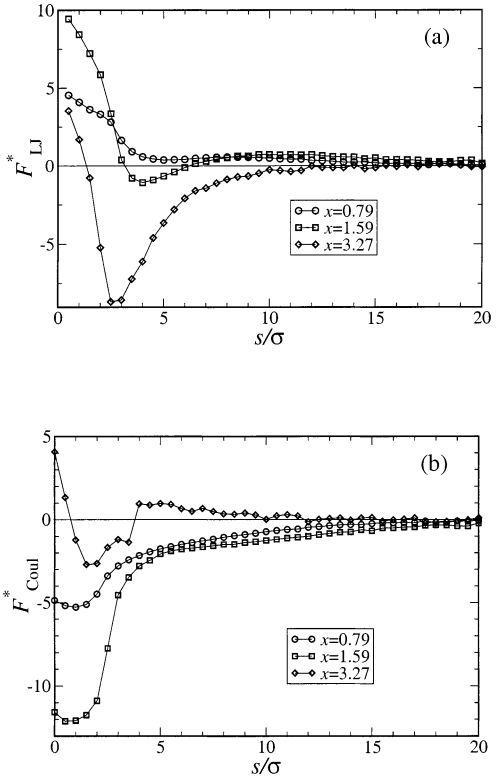

Figure 12. Plot a: simulation results of the entropic part of the force $F^*_{LJ} = \beta\sigma F_{LJ}$ defined in eq 31 for different chain lengths and $z = 1$. The colloid radius is $\tilde{R}_0 = 5.0$. Plot b: simulation results for the Coulombic part of the force $F^*_C = \beta\sigma F_C$ eq 30 using the same parameters as in plot a. Lines are guide to the eye.

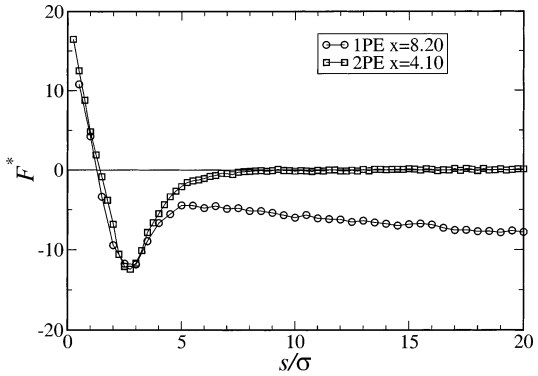

Figure 13. Simulation results of the force between two colloids with $\tilde{R}_0 = 5.0$ carrying two chains of length $x = 4.10$ (squares) and one chain with doubled length $x = 8.20$ (circles). The monomer valence is $z = 1$. Lines are guide to the eye.

the area $A = l\sigma$ of the covering chain with length l and thickness σ, which yields

$$x_c = 2\pi R/\sigma \tag{36}$$

We compared above estimate for two different complex radii $R \approx 3.0$ and $R \approx 6.0$ with simulation results and found $x_c \approx 15$ and $x_c \approx 33$ which is very close to the theoretical results $x_c = 18.85$ and $x_c = 37.70$. See Figure 12b for examples for the force between two complexes with a colloid radius $\tilde{R}_0 = 5$.

C. Effects of Chain Stiffness or Salt. Increasing chain stiffness has an enormous influence on the interaction for all chain lengths. The mechanism of interaction changes completely as now the rigid chains

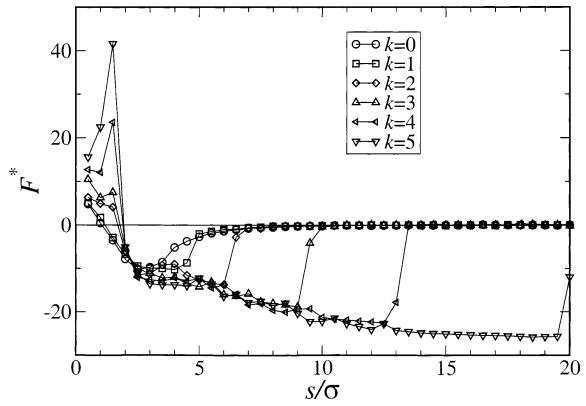

Figure 14. Simulation results of the force between two PE−colloid complexes for a fixed chain length $x = 3.27$, $z = 1$, and different rigidity $k = \beta k_{ang}$ according to eq 15. Lines are guide to the eye.

try to bridge between the colloids to lower their bending energy which now is not negligible as compared to the electrostatic energy. Simulation results for increasing chains stiffness are shown in Figure 14 for a chain length $x = 3.27$. At a critical distance, the chains bridge from one colloid to the other as shown in the snapshot in Figure 7g. We checked that the isolated complex with this length and bonding parameters shows always a complete adsorption of the PE to the charged sphere and no one- or two-tail configurations. The functional behavior of the force is linear for a wide range of the distance. This is similar to the interaction of two colloids with only one chain, see Figure 4 discussed in ref 20 where the sharing of the chain was named energetic bridging as one chain is then able to neutralize both colloids and lower the electrostatic energy. In our similar case with two chains the bridging is due to lowering of the bending energy of the rigid chains.

Adding salt in low concentrations shows no surprising behavior of the interactions for all chain lengths. The shape and qualitative behavior of the force changes hardly and the magnitude of attraction decreases when the salt concentration rises. In Figure 15a, we plot the simulation results for the case of short chains, $x = 1.59$, where the dipole attraction dominates, and in Figure 15b, we plot data for a rather long chain $x = 4.10$ where the major part of the interaction has entropic origin. Notice the disappearance of the very short-range attraction $0 < s \lesssim 3\sigma$ for the short chains already for $c_s \approx 0.07$. Also the long-range dipole interaction is relatively reduced. For the long chain the interaction is hardly affected until the salt concentration reaches values of about $c_s \approx 0.15$ M. Further increasing of the salt concentration weakens the attractive force until desorption of the chain takes place. For the short chain this happens for $c_s > 0.5$ M while for the long chain still attraction occurs up to $c_s \approx 1.7$ M due to the larger total charge in the system.

V. Final Remarks

In summary, we studied the polarizability and interaction of PE−colloid complexes for the case where the chain is fully adsorbed on the macroion. The polarizability is strong for small chains and small electrical fields and has a maximum for chain length comparable to the circumference of the colloid. It can theoretically be described in terms of a thermally fluctuating dipoles with an effective length which depends on the chain

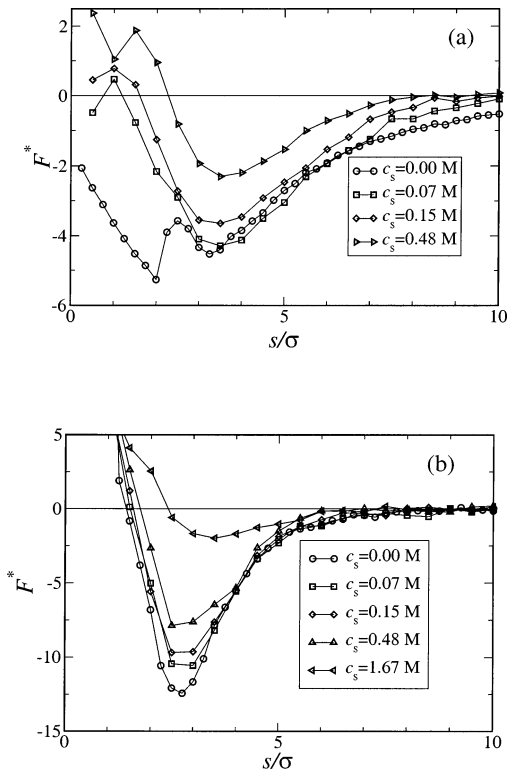

Figure 15. Simulation results of the dimensionless force $F^* = \beta\sigma F$ between two PE−colloid complexes vs the distance s for a fixed chain length (a) $x = 1.57$ and (b) $x = 4.10$ for different salt concentrations c_s.

length. For chains longer than the circumference of the macroion, the polarizability is on the order of the polarizability of a classical conducting sphere with radius of complex size. The interaction shows a van der Waals like attraction for short chains and a deep short-range attraction for midsized chains. When a critical chain length $x_c$is exceeded, the interaction is completely repulsive. One could in principle try to explain the strong short-range attraction seen in the simulations through the attractive interaction seen between equally charged walls in the presence of polyelectrolytes[40] or counterions[41] (using the Derjaguin approximation to correct for the spherical geometry). However, one should note that the Derjaguin approximation is only valid in the limit where the colloidal particle is much larger than the adsorbed chains, which is not the case in the simulations presented here.

One of the interesting conclusions that one can draw from this work concerns the stability of colloidal suspensions which are stabilized by adsorption of polyelectrolytes. While for chains which are very long compared to the size of the particles $x > x_c$ this is indeed an effective mechanism of stabilization (as shown in Figure 6 for $x = 32.79$, where the forces are always repulsive or zero), complexes with chains with a length comparable with the colloidal size exhibit a short-range attraction due to the so-called bridging between the particles. However, for chains that are smaller than the colloid, a long-range attraction is present and one should expect such suspensions to behave like dipolar fluids.[42] This shows that the stabilization of colloidal suspensions by polyelectrolyte adsorption is strongly dependent on the chain size relative to the colloidal size: for long chains the suspensions are always stable (only repulsive forces between the particles), while for midsized and short chains there is attraction between the complexes and a salting-out can occur. Although our studies were essentially done for isolated, strongly charged and symmetric complexes these conclusions should hold in more realistic situations where the chains have some polydispersity and the complexes are at relatively high concentrations, since the only key point is the existence of the complexes.

Acknowledgment. The authors thank H. Löwen and C. Likos for a critical reading of the manuscript. J.D. thanks O. Farago and M. Sabouri-Ghomi for useful discussions. This research was in part supported by the National Science Foundation under Grant No. PHY99-72246 and by the MRSEC program of the NSF under Award No. DMR00-80034. J.D. acknowledges a financial grant from the DAAD Doktorandenstipendium and support from the DFG under "Schwerpunkt Polyelektrolyte".

References and Notes

(1) Kunze, K.-K.; Netz, R. R. *Phys. Rev. Lett.* **2000**, *85*, 4389.
(2) Sakaue, T.; Yoshikawa, K.; Yoshimura, S. H.; Takeyasu, K. *Phys. Rev. Lett.* **2001**, *87*, 078105.
(3) Nguyen, T. T.; Shklovskii, B. I. *J. Chem. Phys.* **2001**, *115*, 7298.
(4) Gelbart, W. M.; Bruinsma, R. R.; Pincus, P. A.; Parsegian, V. A. *Phys. Today* **2000**, *53*, 38.
(5) Wallin, T.; Linse, P. *Langmuir* **1996**, *12*, 305.
(6) Wallin, T.; Linse, P. *J. Chem. Phys.* **1998**, *109*, 5089.
(7) Netz, R. R.; Joanny, J.-F. *Macromolecules* **1999**, *32*, 9026.
(8) Mateescu, E. M.; Jeppesen, C.; Pincus, P. A. *Europhys. Lett.* **1999**, *46*, 493.
(9) Schiessel, H.; Rudnick, J.; Bruinsma, R.; Gelbart, W. M. *Europhys. Lett.* **2000**, *51*, 237.
(10) Nguyen, T. T.; Shklovskii, B. I. *Physica A* **2000**, *293*, 324.
(11) Welch, P.; Muthukumar, M. *Macromolecules* **2000**, *33*, 6159.
(12) Schiessel, H.; Bruinsma, R.; Gelbart, W. M. *J. Chem. Phys.* **2001**, *115*, 7245.
(13) Chodanowski, P.; Stoll, S. *J. Chem. Phys.* **2001**, *115*, 4951.
(14) Jonsson, M.; Linse, P. *J. Chem. Phys.* **2001**, *115*, 3406.
(15) Jonsson, M.; Linse, P. *J. Chem. Phys.* **2001**, *115*, 10975.
(16) Akinchina, A.; Linse, P. *Macromolecules* **2002**, *35*, 5183.
(17) Gurovitch, E.; Sens, P. *Phys. Rev. Lett.* **1999**, *82*, 339.
(18) Nguyen, T. T.; Shklvskii, B. I. *J. Chem. Phys.* **2001**, *114*, 5905.
(19) Park, S. Y.; Bruinsma, R. F.; Gelbart, W. M. *Europhys. Lett.* **1999**, *46*, 454.
(20) Podgornik, R.; Akesson, T.; Jönsson, B. *J. Chem. Phys.* **1995**, *102*, 9423.
(21) Granfeldt, M. K.; Jönsson,; Woodward, C. E. *J. Phys. Chem.* **1991**, *95*, 4819.
(22) Likos, C. N. *Phys. Rep.* **2001**, *348*, 267−439.
(23) Netz, R. R. Manuscript in preparation.
(24) Stevens, M. J.; Kremer, K. *J. Chem. Phys.* **1995**, *103*, 1669.
(25) Grest, G. S.; Kremer, K.; Witten, T. A. *Macromolecules* **1987**, *20*, 1376−1383.
(26) Grest, G. S. *Macromolecules* **1994**, *27*, 3493−3500.
(27) Jusufi, A.; Watzlawek, M.; Löwen, H. *Macromolecules* **1999**, *32*, 4470−4473.
(28) Jusufi, A.; Dzubiella, J.; von Ferber, C.; Likos, C. N.; Löwen, H. *J. Phys.: Condens. Matter* **2001**, *13*, 6177.
(29) Jusufi, A.; Likos, C. N.; Löwen, H. *J. Chem. Phys.* **2002**, *116*, 11011.
(30) Jusufi, A.; Likos, C. N.; Löwen, H. *Phys. Rev. Lett.* **2002**, *88*, 018301.
(31) Essafi, W.; Lafuma, F.; Williams, C. E. *J. Phys. II (Fr.)* **1995**, *5*, 1269.
(32) Hansen, J.-P.; Löwen, H. *Annu. Rev. Phys. Chem.* **2000**, *51*, 209.
(33) Manning, G. S. *J. Chem. Phys.* **1969**, *51*, 924; *J. Chem. Phys.* **1969**, *51*, 934.
(34) Allen, M. P.; Tildesley, D. J. *Computer Simulation of Liquids*; Clarendon Press: Oxford, England, 1987.
(35) Madras, N.; Sokal, A. D. *J. Stat. Phys.* **1988**, *50*, 109.
(36) Dzubiella, J.; Schmidt, M.; Löwen, H. *Phys. Rev. E* **2000**, *62*, 5081.
(37) Jackson, J. D. *Classical Electrodynamics*, 2nd ed.; John Wiley & Sons: New York, 1925.

(38) Keesom, W. H. *Phys. Z.* **1921**, *22*, 129.
(39) Akesson, T.; Woodward, C.; Jönsson, B. *J. Chem. Phys.* **1989**, *91*, 2461.
(40) Ennis, J.; Sjöström, L.; Åkesson, T.; Jönsson, B. *Langmuir* **2000**, *16*, 7116.
(41) Moreira, A. G.; Netz, R. R. *Phys. Rev. Lett.* **2001**, *87*, 078301.
(42) Teixeira, P. I. C.; Tavares, J. M.; de Gama, M. M. T. *J. Phys., Condens. Matter* **2000**, *12*, R411.

MA021322L